



## Assessment of soil compaction and rutting in managed forests through an airborne LiDAR technique

Hamza Mohieddine, Boris Brasseur, Emilie Gallet-Moron, Jonathan Lenoir,  
Fabien Spicher, Ahmad Kobaissi, Hélène Horen

### ► To cite this version:

Hamza Mohieddine, Boris Brasseur, Emilie Gallet-Moron, Jonathan Lenoir, Fabien Spicher, et al..  
Assessment of soil compaction and rutting in managed forests through an airborne LiDAR technique.  
Land Degradation and Development, 2022, 34 (5), pp.1558-1569. 10.1002/ldr.4553 . hal-04007808

**HAL Id: hal-04007808**




**<https://u-picardie.hal.science/hal-04007808>**

Submitted on 12 Jun 2023

**HAL** is a multi-disciplinary open access archive for the deposit and dissemination of scientific research documents, whether they are published or not. The documents may come from teaching and research institutions in France or abroad, or from public or private research centers.

L'archive ouverte pluridisciplinaire **HAL**, est destinée au dépôt et à la diffusion de documents scientifiques de niveau recherche, publiés ou non, émanant des établissements d'enseignement et de recherche français ou étrangers, des laboratoires publics ou privés.

# Assessment of soil compaction and rutting in managed forests through an airborne LiDAR technique

Hamza Mohieddinne<sup>1,2</sup>  | Boris Brasseur<sup>1</sup>  | Emilie Gallet-Moron<sup>1</sup> |  
Jonathan Lenoir<sup>1</sup>  | Fabien Spicher<sup>1</sup> | Ahmad Kobaissi<sup>3</sup> | H       Horen<sup>1</sup>

<sup>3</sup>Applied Plant Biotechnology Laboratory (APBL), Faculty of Sciences, Lebanese University, Hadath, Lebanon

Hamza Mohieddinne, INRAE Centre de Nancy  
Grand-Est, Rue d'Amance, 54280  
Champenoux, France.  
Email: [hamzemohieddin@gmail.com](mailto:hamzemohieddin@gmail.com)

To ensure sustainable forest management, the assessment and monitoring of soil compaction and rutting are essential. Here, we used airborne light detection and ranging-derived digital terrain model (LiDAR-derived DTM), available for the forest of Compiègne in northern France, to compute a spatial index of soil rutting. Following an environmental systematic sampling design, we selected 45 plots representative of the forest stand conditions where we subsequently extracted information from the DTM to compute the cumulative length of ruts (CLR). To assess the quality of this LiDAR-derived index, we related the CLR index to in-situ soil and vegetation parameters such as soil texture, soil pH, and understory plant species composition. Floristic surveys were carried out across all 45 plots to generate plant species response curves along the CLR gradient. We found soil texture, soil type, and soil pH to be important determinants of CLR. For instance, CLR was the highest in soils with the highest clay content. A total of 22 out of the 94 understory plant species we analyzed showed a significant response curve along the CLR gradient. Most important, the occurrence probability of species associated with wet soils and stagnant waters (e.g., *Juncus effusus*), like those found in ruts, increased with CLR. Other species associated with dry soils (e.g., *Hedera helix*) showed a negative response curve along the CLR gradient. In conclusion, the proposed index (CLR) has proven useful to remotely assess soil compaction and rutting after logging operations.

airborne LiDAR, forest management, remote sensing, soil compaction and rutting, species response curves

Forest management practices contribute to the alteration of ecosystem functioning, chiefly through soil compaction and rutting (Grigal, 2000). Nowadays, forest managers are facing the challenge to meet the societal demand for wood and non-wood forest products while complying with the sustainable use of forest resources (Camb

et al., 2015). The long-term effects of logging operations on forest soils (e.g., compaction) due to the increasing implementation of forest mechanization urges the need to develop rutting reduction measures for economical and ethical reasons (Grigal, 2000). Traffic of heavy machines generates mechanical stress on forest soils, often exceeding the soil bearing capacity, which leads to the formation of ruts on the soil surface (Hillel, 2004a; Horn et al., 2007). Even the deep soil

© 2022 The Authors. *Land Degradation & Development* published by John Wiley & Sons Ltd.

structure is affected by the reduction of soil porosity and the increase of soil compaction and penetration resistance (Cambi et al., 2015; Mohieddinne et al., 2019). Such structural collapses in soils are known to decrease gas exchanges at the interface between the soil and the atmosphere, and to reduce the infiltration of water in the deep soil layers (Ampoorter et al., 2010), enhancing water accumulation at the soil surface (e.g., stagnant waters in ruts). In general, soil compaction leads to a decrease in the mineralization activities in soils and to a reduction of the bioavailability of essential elements, potentially reducing soil fertility (Arocena, 2000). These alterations hinder water uptake, oxygen supply, seedling and germination success, as well as root development (Brajs, 2001; Cambi, Giannetti, et al., 2018; Greacen & Sands, 1980; Hamza & Anderson, 2005; Pardo et al., 2000; Schumacher & Smucker, 1981). Consequently, it leads to a decreased photosynthesis rate, growth, and regeneration of the forest overstory (Blouin et al., 2008; Cambi et al., 2017; Slesak & Kaebisch, 2016). The recovery time of compacted soil structures is known to take several decades, but it will never come back to the initial state (Ebeling et al., 2016; Goutal et al., 2012; Meyer et al., 2014; Mohieddinne et al., 2019). The long-term impact of soil compaction and rutting led forest managers worldwide to search for mitigation strategies to reduce this impact. For instance, limiting the surface affected by the traffic of heavy forest vehicles is one of these mitigating strategies. By establishing a designated network of permanent skid trails over which the traffic should be carried out, forest managers would be able to reduce the impacted surfaces by about 60% (Augoyard et al., 2017).

Noteworthy, the increase of soil moisture and water accumulation in ruts, due to poor water infiltration rate in the deeper soil layers, benefits the occurrence and local abundance of several plant species typically associated with soil compaction and stagnant waters, chiefly wetland and ruderal plants (e.g., *Juncus effusus* and *Rumex sanguineus*) (Kozłowski, 1999; Wei et al., 2015; Weltecke & Gaertig, 2011). Those indicator species are enhanced by soil compaction (Godefroid & Koedam, 2004a; Perry et al., 2008; Weltecke & Gaertig, 2011) and compete with the other vegetation for access to soil nutrients, even contributing to the reduction of seedling establishment success (Kozłowski, 1999). Godefroid and Koedam (2004a) have studied the response of understory forest herbs to soil compaction and reported highly significant increases in the abundance of wetland and ruderal species. In addition, forest and paths' network, including ruts, increase the number of ruderal plants (e.g., *Agrostis stolonifera*, *Geum urbanum*, *Rumex sanguineus*) as well as other species indicating forest disturbances by heavy machines (Avon et al., 2013; Godefroid & Koedam, 2004b). Mercier et al. (2019) showed that skid trails favour rich, light, and moisture-demanding species that are spatially confined to the trails.

The level of soil compaction and rutting are usually measured in-situ, using field equipment and observations. Rutting is typically measured as the depth of the ruts, which is potentially time-consuming if rutting is measured across large spatial extents (Koreň et al., 2015). Soil physical (e.g., bulk density, penetration resistance, shear strength), physicochemical (e.g., redox potential, pH), and biological (e.g., CO<sub>2</sub> efflux, microbe activity) parameters describe the alteration level of the soil after compaction. These properties can also be measured directly in-situ or in the lab based on soil samples, which does not necessarily optimize the time spent

to evaluate soil alteration, especially across large spatial extents. Recent scientific advances in remote sensing provide a promising, although largely untapped, resource for a spatially and temporally standardized monitoring of soil compaction and rutting in forest systems. Indeed, there is a strong need to develop methods and approaches relying on remote sensing to help and guide forest managers to limit the negative impacts of forest mechanization on forest soils. Recently, numerous studies highlighted the promising efficiency of remote sensing in the assessment of soil rutting (Cambi et al., 2018; Niemi et al., 2017; Pierzchała et al., 2016; Salmivaara et al., 2018). Some of them used high-resolution photogrammetry to assess soil rutting after forest harvesting (Haas et al., 2016; Pierzchała et al., 2016). Cambi et al. (2018) reported, across a limited spatial extent, that high-resolution photogrammetry could be used to derive proxies of soil compaction that are representative of in-situ measurements. The same technology was used by Marra et al. (2018) who found a strong correlation between manual measurements carried out in the field and the outcomes from high-resolution photogrammetry. Similarly, Talbot et al. (2018) used unmanned aerial vehicles (UAVs) equipped with digital cameras, generating 3D images, to characterize the soil rutting severity after forest harvesting. Yet, such an approach based on UAVs is only applicable over recently clear-cut/harvested areas and across relatively small spatial extents. Alternatively, terrestrial laser scanning (TLS) using light detection and ranging technology (LiDAR) has been suggested as an alternative to map soil compaction and rutting from below the canopy (Koreň et al., 2015). Still, such an approach is limited by the spatial extent that can be covered using TLS in the field. Airborne LiDAR (i.e., LiDAR sensors on board of aircraft flying above the forest canopy) appears as the best alternative for assessing soil compaction and rutting below the forest canopy and across large spatial extents (Niemi et al., 2017). Despite the accuracy of airborne LiDAR images, it has rarely been used so far to assess soil compaction and rutting, except for the work of d'Oliveira et al. (2012), Niemi et al. (2017) and Callesen et al. (2020) who mapped rutting trails from LiDAR-derived digital elevation and terrain models. Here, we propose to use a digital terrain model (DTM) derived from airborne LiDAR images acquired across a very large afforested area (14,000 ha) to build a rutting index based on the cumulative length of ruts (CLR). We subsequently related CLR to in-situ soil and substrate conditions within the forest (e.g., soil type, soil texture, soil pH, and geological substrate) as well as other determinants related to forest stand characteristics (e.g., stand dominant species and stand age) to assess whether or not it really captures soil rutting and compaction impacts. As for the mitigation strategies mentioned earlier, we also tested whether CLR is lower or not on those sites with permanent skid trails as opposed to other sites without permanent skid trails. Finally, we related CLR to the occurrence of understory plants to investigate its usefulness in remotely detecting the vegetation associated with ruts.

## 2 | MATERIALS AND METHODS

### 2.1 | Study site and sampling design

The study was conducted in the forest of Compiègne, located in northern France (49°22'N; 2°54'E) and characterized by a temperate

climate: 619 mm of mean annual precipitation and 10.5°C in mean annual temperature (Climate-data.org, 2019). This large forest (ca. 14,000 ha) covers a vast plain and several small mounts or plateaus towards the eastern and southern edges, with an elevation gradient ranging from 30 to 148 m above sea level. The geological substrate mainly consists of Paleocene to Eocene, sand, and limestone, locally covered by Quaternary loess or drift sands (BRGM, 2000). The three dominant soil groups are Cambisol, Luvisol, and Podzol (IUSS Working Group WRB, 2015). The forest is a state forest managed by the French National Forest Office (ONF). The current vegetation is a temperate deciduous forest dominated by common beech (*Fagus sylvatica* L.) and oaks (*Quercus robur* L. and *Quercus petraea* Liebl.), with several management units locally dominated by scots pine (*Pinus sylvestris* L.) (ONF, 2012). Forest management practices as well as mitigation strategies to limit soil compaction inside management units of the forest are detailed in Mohieddinne et al. (2019). A total of 45 plots were selected across the study area (Figure 1a) following an environmental systematic sampling design that maximizes the variability of environmental and stand conditions available throughout the forest (see Hattab et al., 2017). Floristic surveys were performed during the summer of 2017 to record all vascular plants (e.g., ferns, grasses, herbs, sedges, and seedlings) co-occurring inside the herbaceous layer (below 1-m height) of a circular surface area of 400 m<sup>2</sup> covering each of the 45 studied plots.

## 2.2 | A LiDAR-derived measure of soil rutting (CLR)

Airborne LiDAR images were acquired on February 2014 at leaf-off conditions by the Aerodata Company (Lille, France) using a Riegl LMS-680i with a minimum point density of 12 pts per m<sup>2</sup>, a maximum scan angle of 30° and a lateral overlap between neighboring flight lines of 65%. Average flight height during LiDAR data acquisition was 530 m resulting in a beam diameter of about 0.265 m when projected on the ground. The LiDAR data as delivered by the Aerodata Company included a classification of ground and vegetation returns as well as a digital terrain model (DTM), at 50-cm of resolution, generated from the ground points (Figure 1b). From the DTM, we ran a local relief model (LRM) to help visualize the small-scale topographic variations (Hesse, 2010) allowing us to highlight the ruts of logging paths (Figure 1c). The LRM process removes the large-scale landscape features from the data to present local and small-scale elevation differences (Hesse, 2010). Based on the images generated by the LRM, we manually digitized the revealed skid trails in a geographical information system (GIS) (Figure 1d). Then, we overlapped the digitized skid trails (i.e., polylines) with the 45 plots to compute the cumulative length of ruts (CLR) inside the 400 m<sup>2</sup> surface area of each plot.

As part of the forest management plan, the implementation of permanent skidding trails within forest management units (FMUs) is adopted to limit and reduce the formation of ruts. When regular and

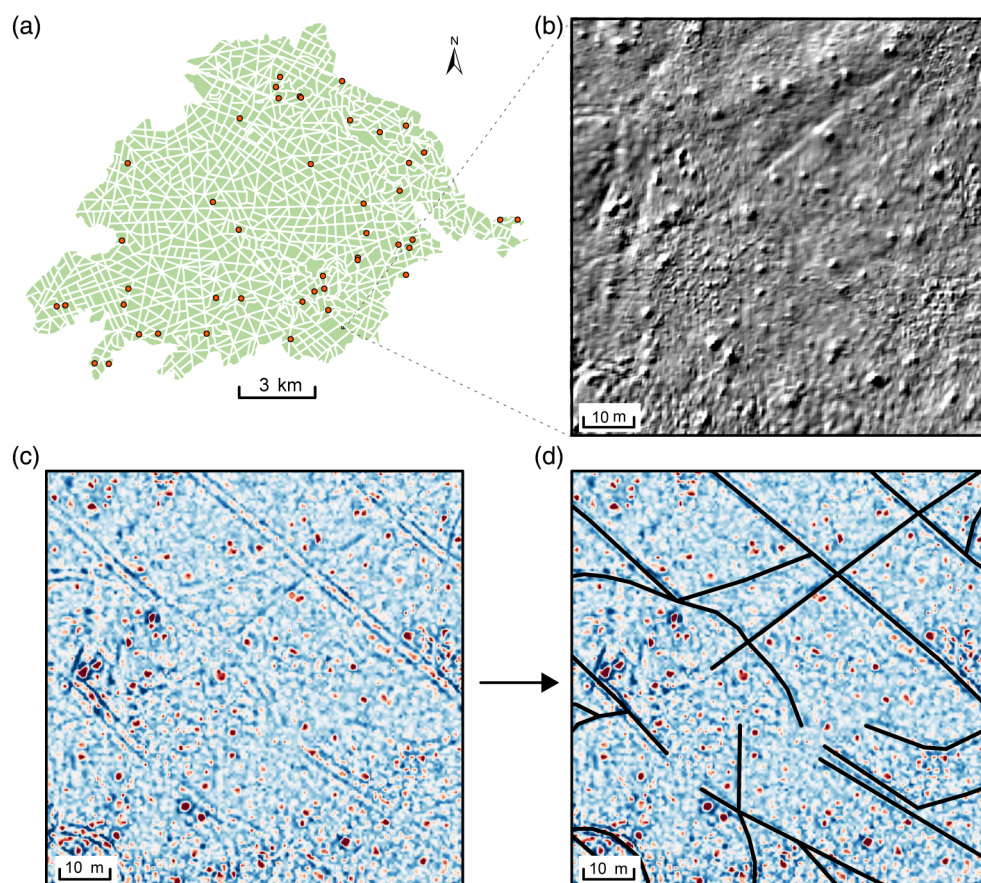


**FIGURE 1** The study area. Spatial distribution of the 45 studied plots across the forest of Compiègne (a). Zooming window on one of the 45 study plots depicting: the light detection and ranging (LiDAR)-derived digital terrain model (DTM) (ruts are displayed by shading) (b); the local relief model (LRM) which highlights the trails of compaction as linear sunken paths (c); and the digitization of the compaction trails to calculate the cumulative length of ruts (CLR) (d) [Colour figure can be viewed at [wileyonlinelibrary.com](https://onlinelibrary.wiley.com/terms-and-conditions)]



parallel-spaced ruts were observed on LiDAR images, we assumed these were from permanent skidding trails belonging to the focal FMU, as planned by forest managers. Yet, in many FMUs throughout the forest, the LRM revealed meandering skidding trails that are not permanent but opportunistic, which increases the surface area covered by ruts throughout the forest. Thus, we classified the studied plots into two categories: those only crossed by permanent and regular skidding trails versus those crossed by non-permanent and irregular skidding trails.

All spatial and geographical analyses were performed using QGIS 2.18 Las Palmas.

### 2.3 | Management, substrate, and stand conditions effects on CLR

First, we performed a Student *t*-test to compare the mean CLR between plots only crossed by permanent skidding trails and plots crossed by non-permanent skidding trails to assess whether CLR is higher in plots crossed by non-permanent skidding trails. Second, we aimed at testing the impact of substrate conditions (soil pH, soil type, soil texture, and geological substrate) and stand characteristics (dominant tree species and stand age) on CLR. Because the CLR variable follows a Normal distribution, we used an ordinary least square regression (OLS) to test the relative influence of substrate conditions and stand characteristics (i.e., the set of explanatory variables) on CLR (i.e., the response variable). All explanatory variables, except stand age and soil pH, are categorical variables: soil type has four levels (Cambisol, Luvisol, Podzol, and Gleysol); soil texture also has four levels (clayey sand, high sandy loam, loamy sand, and sand); geological substrate has six levels (alluvium, calcareous, colluvium, sand, silt, and the last level grouping clay, lignites, and faluns together); and the dominant tree species has five levels (beech, oak, scots pine, other broadleaf species, and other coniferous species). Based on the rather small sample size of our dataset ( $n = 45$  plots), we could only test for a few candidate models consisting of none (identity model) to four explanatory variables without testing for all interaction effects here. Only the interaction between soil type and pH was tested. All possible combinations from none to four explanatory variables were tested, leading to a total of 42 candidate models. The potential redundancy (i.e., multi-collinearity issues) between the six studied explanatory variables was also assessed, and some variables were excluded from the candidate models when redundancy was detected, such as between geological substrate and soil texture, which are highly correlated. The Akaike information criterion (AIC), corrected for small sample sizes (AICc), was adopted to select the best candidate model, which is the one with the lowest AICc value (Table A1.1 in the Appendix) (Burnham & Anderson, 2002; Hurvich & Tsai, 1989). The analysis of variance, two-way ANOVA, was performed on the best candidate model. In addition, variation partitioning was carried out on the best candidate model to describe how much variation was explained by each of the explanatory variables involved in the best candidate model.

### 2.4 | Does CLR relate to understory plant species distribution?

Here, we aimed at testing the ability of our LiDAR-derived CLR index to predict the distribution of understory plant species and more specifically whether or not understory plants associated with wet soils and stagnant waters in ruts are positively responding along the CLR gradient. To capture the spectrum of local conditions covered by understory plants associated with ruts, we used Ellenberg indicator values (EIVs) for soil moisture (F), soil nutrient conditions (N), light (L), and soil reaction (R) (Mueller-Dombois & Ellenberg, 1974). For instance, wetland plants tend to have high EIVs along the F gradient ranging from 1, for plants associated with dry soils, to 12, for plants associated with aquatic underwater conditions, through 5–9 for plants associated with moist and wet conditions. Hence, depending on soil type and soil texture (i.e., sandy soils are less likely to generate ruts with standing waters), most of the understory plant species occurring in or close to ruts with standing waters should have high F EIVs, between 5 and 10. To test this hypothesis, we computed the mean of EIVs for F across all vascular plant species that are co-occurring within each of the 45 plots (EIV-F). Then we related this community-based metric to CLR, assuming a positive correlation. Likewise, soil compaction affects negatively soil fertility (EIV-N) and soil reaction (EIV-R). Hence, we assumed a negative correlation between CLR and EIV-N as well as between CLR and EIV-R. Logging operations also increase light conditions near the ground surface due to the opening of the upper canopy layer. Because of that, we assumed a positive correlation between CLR and EIV-L. As an alternative metric of canopy opening, we also computed canopy density from the raw LiDAR point cloud and assumed a negative correlation between CLR and canopy density. Additionally, we assumed plant-specific richness (SR) within each plot to increase with CLR, due to the micro-topography generating micro-climatic conditions that may enhance the occurrence of wetland, ruderal, and light-demanding species throughout the transport of seeds by forest vehicles (Avon et al., 2013; Beatty, 1984; Mercier et al., 2019).

Finally, for each species occurring in at least 10% of the plots and less than 90% of the plots (being a total of 94 species occurring in 5–40 plots), we modelled the response curve of the species' occurrence probability along the CLR gradient. We had to exclude rare species occurring in less than five plots or very common species occurring on almost all of the 45 studied plots to be able to fit a model and thus a species response curve along the CLR gradient. For each of the 94 selected species, we fitted generalized linear models (GLMs) using a binomial family (i.e., logistic regression) to match the distribution of the response variable being binary (i.e., each species presence/absence). As for the explanatory variables, we used CLR as the main predictor variable as well as four other covariates to account for potential confounding effects with CLR. Indeed, the amount of light reaching the ground surface (sunshine) as well as soil conditions (soil pH, soil type, and soil texture) will affect the distribution of understory plants such that it could be confounded with the CLR gradient. Therefore, for each species, seven candidate models were tested: (i) CLR

+ sunshine + pH + soil type; (ii) CLR + sunshine + pH + soil texture; (iii) CLR + soil texture; (iv) CLR + sunshine; (v) CLR + pH; (vi) CLR + soil type; and (vii) CLR only. The model showing the lowest AICc was selected as the best candidate model. For each species showing a significant relationship with CLR, being positive or negative, we generated the response curve or probability of occurrence along the range of values covered by the CLR index throughout our study area. We assumed a positive effect of the CLR variable on the probability of occurrence for species with high F values (i.e., species associated with wet conditions) but a negative effect for species with low F values (i.e., species associated with dry soils).

All statistical analyses were performed using the R software environment (R Development Core Team, 2016) and significance was assessed at a level of  $p$ -value  $\leq 0.05$ .

### 3 | RESULTS

#### 3.1 | The impact of soil conditions on the rutting index

Within our study area, we found the cumulated length of ruts (CLR) to range from 0 to 124.5 m (mean  $\pm$  SEM =  $66.3 \pm 5.2$ ). The mean CLR value in forest management units (FMUs) with permanent skidding trails (mean  $\pm$  SEM =  $91.35 \pm 9.6$ ,  $N = 9$ ) was significantly higher ( $p$ -value = 0.01) than the mean CLR value in FMUs without permanent skidding trails (mean  $\pm$  SEM =  $61.75 \pm 1.82$ ,  $N = 35$ ) (Figure AI.1 in the Appendix). The best model explaining the observed variation in CLR included four explanatory variables: soil pH; soil type; soil texture; and the stand dominant species (Table AI.1, model m23, in the Appendix). This model explained 32% of the total variation for CLR ( $R^2 = 0.5$ ,  $R^2_{adj} = 0.32$ ). The analysis of variance in this model (Table AI-3 in the Appendix) showed a significant effect on soil type, soil texture, and soil pH ( $p$ -value = 0.008, 0.006, and 0.043, respectively). The variation partitioning showed that 25% of the total variation of CLR is explained by the soil texture, 8% by the soil pH, 8% by the dominant tree species in the stand, and 4% by the soil type. Then, 5% of the total variation was explained by the overlap between the

dominant tree species and soil pH, 3% by the overlap between soil pH and soil type, 3% by the overlap between the dominant tree species and soil type, 1% by the overlap between soil texture and soil type, and finally 1% by the overlap between soil pH and soil type. The fitting model of CLR (i.e., m23 in Table AI.1 in the Appendix) showed a significant decrease of CLR on sandy loam ( $p$ -value = 0.01), loamy sand ( $p$ -value = 0.001), and sand ( $p$ -value = 0.001) textures compared to the clayey sand texture used as a reference in the model (cf. the intercept). We also found a significant decrease in CLR with the increase in soil pH ( $p$ -value = 0.04). According to stand characteristics, we found the CLR index to be significantly higher in plots dominated by scots pine ( $p$ -value = 0.028) than in plots dominated by beech. For soil types, the CLR index was lower on Gleysols but higher on Luvisols compared to Cambisols as a reference (cf. the intercept) ( $p$ -value = 0.003 and 0.08 respectively) (see Table AI-2 in the Appendix).

#### 3.2 | How does the rutting index relate to understory plants?

As shown in Table 1, none of the variables derived from the floristic surveys at the community level, like Ellenberg Indicator Values (EIVs) for soil moisture (F) and species richness (SR), were correlated with CLR, while canopy density was negatively correlated to CLR ( $p = -0.36$ ;  $p < 0.01$ ). Irrelatively to CLR, SR was positively correlated with EIV-L, EIV-N, and EIV-R ( $p = 0.3$ , 0.55, and 0.5, respectively) while EIV-R was positively correlated to EIV-N ( $p = 0.48$ ) and canopy density was negatively correlated to EIV-L ( $p = -0.66$ ).

Among the 94 studied plant species for which we studied the response curve along the CLR gradient, 51 species had CLR as the only explanatory variable retained in the best candidate model. Twelve out of 51 had a significant relationship, either positive or negative, with CLR. Additionally, 10 other species showed a significant relationship with CLR as well as another covariate such as soil pH, which makes a total of 22 species showing a significant relationship with CLR (Table 2). Eleven out of 22 species had a significantly positive ( $p$ -value  $\leq 0.05$ ) response curve (i.e., positive sigmoidal shape) along the CLR gradient (*Agrostis stolonifera*, *Carex pendula*, *Carex*

**TABLE 1** Correlation values between the index of cumulative length of ruts (CLR), plant community mean Ellenberg indicator values for light (EIV-L), soil moisture (EIV-F), soil reaction (EIV-R), soil fertility (EIV-N), species richness (SR), and canopy density

	CLR	SR	EIV-L	EIV-F	EIV-R	EIV-N	Canopy density
CLR	1						
SR	0.01 <sup>NS</sup>	1					
EIV-L	0.000305 <sup>NS</sup>	0.3*	1				
EIV-F	0.2 <sup>NS</sup>	0.06 <sup>NS</sup>	-0.03 <sup>NS</sup>	1			
EIV-R	0.08 <sup>NS</sup>	0.55***	0.17 <sup>NS</sup>	0.09 <sup>NS</sup>	1		
EIV-N	0.19 <sup>NS</sup>	0.5***	0.01 <sup>NS</sup>	0.09 <sup>NS</sup>	0.48***	1	
Canopy density	-0.36*	0.04 <sup>NS</sup>	-0.66***	-0.07 <sup>NS</sup>	0.02 <sup>NS</sup>	0.09 <sup>NS</sup>	1

Note: NS corresponds to a non-significant correlation, \* corresponds to a significance level at  $p \leq 0.05$  \*\* corresponds to a significance level at  $p \leq 0.01$ , and \*\*\* corresponds to a significance level at  $p \leq 0.001$ .

**TABLE 2** Descriptive statistics of the best candidate models selected to generate species response curves along the studied gradient of cumulative length of ruts (CLR). Only species having a significantly positive or negative relationship with CLR are listed here

Species	Explanatory factor	Coefficient estimate	Standard error	z-value	p-value
<i>Agrostis stolonifera</i>	Intercept	−4.70	1.51	−3.12	0.0018
	CLR	0.04	0.02	2.49	0.0129
<i>Carpinus betulus</i>	Intercept	2.11	0.81	2.59	0.0095
	CLR	−0.03	0.01	−2.59	0.0097
<i>Carex digitata</i>	Intercept	11.64	5.27	2.21	0.0273
	CLR	−0.05	0.02	−2.12	0.0345
	pH	−1.94	0.85	−2.29	0.0221
<i>Carex flacca</i>	Intercept	7.04	3.88	1.82	0.0692
	CLR	−0.04	0.02	−2.25	0.0245
	pH	−1.07	0.58	−1.84	0.0656
<i>Carex pendula</i>	Intercept	−3.68	1.11	−3.31	0.0009
	CLR	0.04	0.01	3.04	0.0024
<i>Carex remota</i>	Intercept	−3.62	1.20	−3.02	0.0025
	CLR	0.03	0.01	2.20	0.0281
<i>Circaea lutetiana</i>	Intercept	−0.86	0.70	−1.23	0.2184
	CLR	0.02	0.01	2.10	0.0357
<i>Convallaria majalis</i>	Intercept	0.11	0.86	0.13	0.8948
	CLR	−0.04	0.02	−2.15	0.0313
<i>Epilobium hirsutum</i>	Intercept	−4.41	1.87	−2.36	0.0183
	CLR	0.04	0.02	1.91	0.0500
	sunshine	−0.49	0.41	−1.20	0.2298
<i>Eupatorium cannabinum</i>	Intercept	−6.06	2.07	−2.93	0.0034
	CLR	0.05	0.02	2.41	0.0160
<i>Festuca heterophylla</i>	Intercept	9.90	4.48	2.21	0.0270
	CLR	−0.04	0.02	−2.11	0.0350
	pH	−1.63	0.71	−2.31	0.0209
<i>Fraxinus excelsior</i>	Intercept	12.99	4.40	2.95	0.0031
	CLR	−0.04	0.02	−2.82	0.0049
	pH	−1.78	0.63	−2.82	0.0048
<i>Fragaria vesca</i>	Intercept	6.41	4.35	1.47	0.1405
	CLR	−0.04	0.02	−2.06	0.0397
	pH	−1.01	0.65	−1.55	0.1209
<i>Glechoma hederacea</i>	Intercept	−2.55	0.90	−2.82	0.0048
	CLR	0.02	0.01	2.23	0.0258
<i>Hedera helix</i>	Intercept	8.13	3.07	2.65	0.0081
	CLR	−0.03	0.01	−2.59	0.0096
	pH	−0.82	0.43	−1.89	0.0582
<i>Juncus effusus</i>	Intercept	−7.30	2.45	−2.98	0.0029
	CLR	0.08	0.03	2.96	0.0031
	soil type Gleysol	6.81	2.68	2.54	2.5430
	soil type Luvisol	1.26	1.03	1.23	0.2202
	soil type Podzol	−2.32	1.73	−1.35	0.1788
<i>Luzula forsteri</i>	Intercept	1.97	0.99	1.20	0.0467
	CLR	−0.04	0.01	−0.64	0.0083
	sunshine	−0.41	0.18	−2.23	0.0258

(Continues)

TABLE 2 (Continued)

Species	Explanatory factor	Coefficient estimate	Standard error	z-value	p-value
<i>Oxalis acetosella</i>	Intercept	−8.62	3.33	−2.59	0.0096
	CLR	0.03	0.02	2.14	0.0327
	pH	0.76	0.45	1.68	0.0938
<i>Quercus petraea</i>	Intercept	0.81	0.75	1.08	0.2815
	CLR	−0.03	0.01	−2.47	0.0136
<i>Solanum dulcamara</i>	Intercept	−3.39	1.15	−2.96	0.0031
	CLR	0.03	0.01	2.05	0.0399
<i>Rumex sanguineus</i>	Intercept	−24.29	3734.66	−0.01	0.9948
	CLR	0.05	0.02	2.25	0.0248
<i>Viola reichenbachiana</i>	Intercept	0.91	0.99	0.92	0.3569
	CLR	−0.04	0.02	−2.28	0.0229

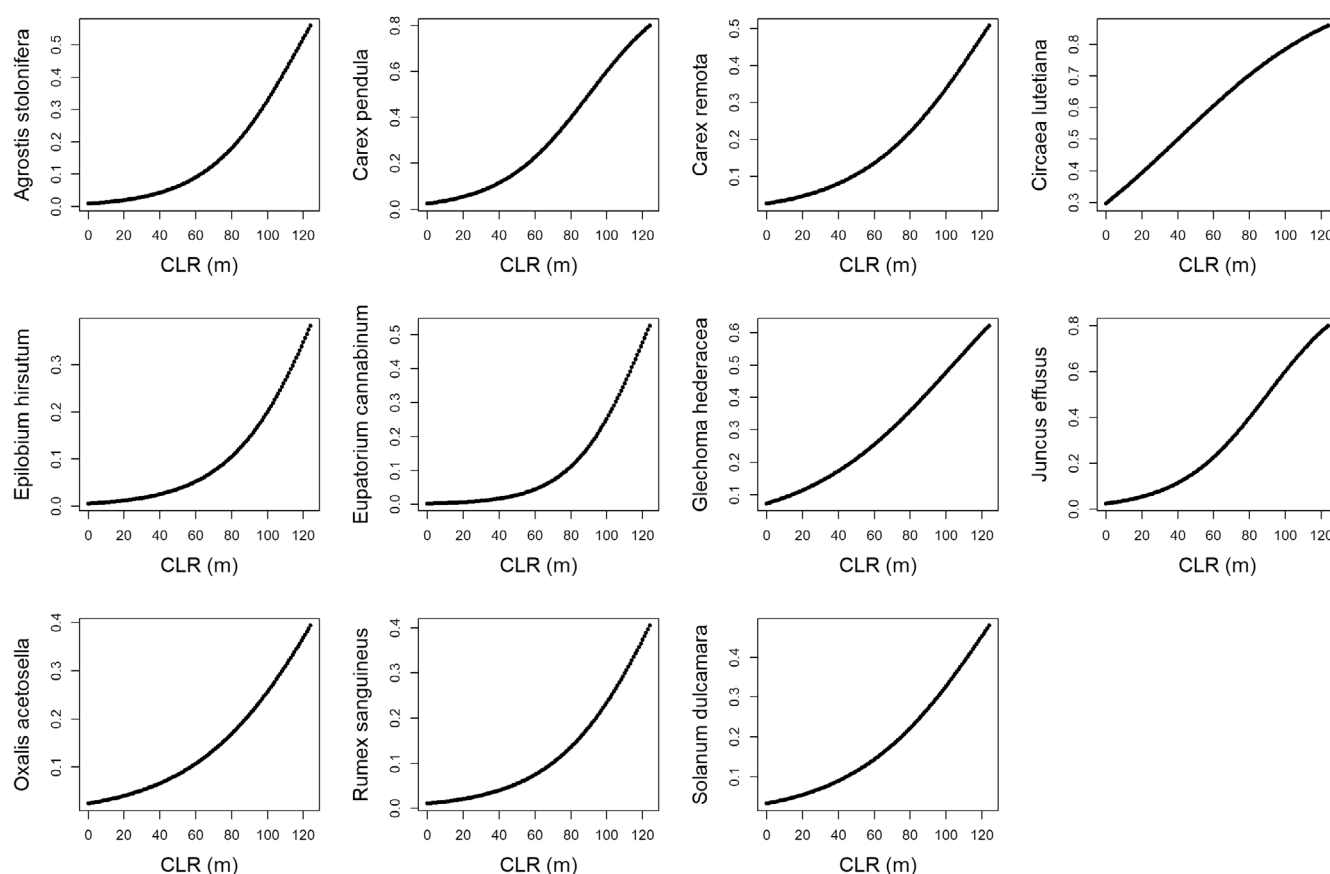


FIGURE 2 Example of understory plant species depicting a significantly positive response curve along the CLR gradient

*remota*, *Circaea lutetiana*, *Epilobium hirsutum*, *Eupatorium cannabinum*, *Glechoma hederacea*, *Juncus effusus*, *Oxalis acetosella*, *Rumex sanguineus*, and *Solanum dulcamara*) (Figure 2). In contrast, the other 11 species had a significantly negative ( $p$ -value  $\leq 0.05$ ) response curve (i.e., negative sigmoidal shape) along the CLR gradient (*Carpinus betulus* seedlings, *Carex digitata*, *Carex flacca*, *Convallaria majalis*, *Festuca heterophylla*, *Fraxinus excelsior* seedlings, *Fragaria vesca*, *Hedera helix*, *Luzula forsteri*, *Quercus petraea* seedlings, and *Viola reichenbachiana*) (Figure 3).

## 4 | DISCUSSION

### 4.1 | What does the rutting index say about the impact of logging operations?

As suggested by others previously (Andersen et al., 2014; Callesen et al., 2020; d'Oliveira et al., 2012; Koreň et al., 2015; Niemi et al., 2017; Salmivaara et al., 2018), we showed that it is indeed possible to assess soil rutting across an entire forest using airborne LiDAR



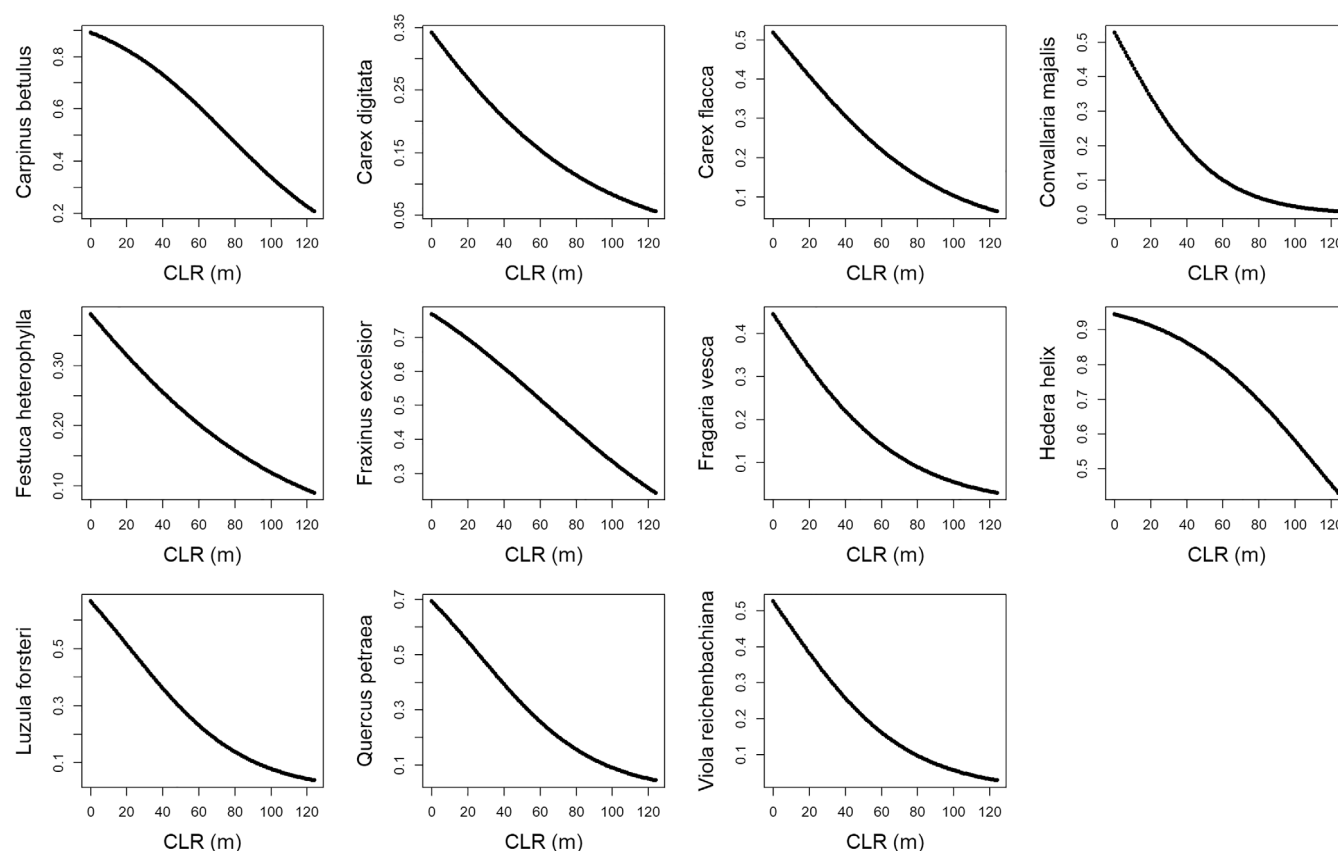


**FIGURE 3** Example of understory plant species depicting a significantly negative response curve along the CLR gradient

data. Using the LRM treatment on a LiDAR-derived DTM at a very high spatial resolution (50 cm resolution), we were able to reveal ruts on the forest floor and below the tree canopy. Based on the LRM, our measure of the rutting (CLR) offers a reliable index to assess soil rutting and thus compaction through remote sensing, with CLR reaching, on average across the studied forest, about 66 m within a circular surface area of 400 m<sup>2</sup>. To extrapolate the total surface impacted by rutting, we should consider the width of the machines' wheels (about 0.7 m on average). Considering this, the total surface area impacted per unit of the area should be about 23%, on average. However, the actual surface impacted by the forestry machines is even greater than that if we consider the bulges of soil generated on the outer sides of the ruts and the space between the two parallel ruts left by the vehicles (Ampoorter et al., 2010; Jansson & Johansson, 1998; Koreň et al., 2015). Hence, the actual bandwidth affected by linear ruts is around 3.5–4 m. Consequently, the average proportion of surfaces impacted by soil rutting may be estimated to reach about 57% of the entire forest of Compiègne.

Contrary to our assumption, our results highlighted higher CLR within FMUs with permanent skidding trails established by forest managers, compared to the other FMUs without any marking of permanent skidding trails. The establishment of permanent skidding lines by forest managers aims at ensuring that forestry vehicles will only use those permanent skidding lines during logging operations and limit the exploration beyond them (Zenner & Berger, 2008). The FMUs

with designated permanent skidding trails should theoretically decrease the proportion of rutted surfaces by circa 60% (Augoyard et al., 2017), which is not what we found. Two hypotheses may explain this unexpected result. First, many studies have demonstrated the persistence of ruts over a very long time after skidding operations (Ebeling et al., 2016; Mohieddinne et al., 2019), which suggests that some ruts, still visible on LRM images, may actually result from logging operations older than the establishment of permanent skidding trails. Second, drivers of forest harvesters may, sometimes, disregard the network of permanent skidding trails for several reasons (poor indication, poor accessibility, etc.). The disregard of a poorly marked network of permanent skidding trails may increase the proportion of rutted surfaces within FMUs with permanent skidding trails compared with FMUs without permanent skidding trails. The network of permanent skidding trails in the forest of Compiègne has been initiated by the ONF during the 1980s (Mohieddinne et al., 2019). We found that the actual network of permanent skidding trails represents about 20% of the studied FMUs, which is much lower than the proportion initially scheduled (ca., 80%) by forest managers in the management plan (provided by the ONF) for the forest of Compiègne. Mohieddinne et al. (2019) mentioned that skidders traffic outside designated skidding trails within forest FMUs that are readily equipped with permanent skidding trails. This means that designated skidding trails are disregarded by logging operators on a significant part of the FMUs during logging operations with skidders going beyond the designated

permanent skidding trails. Therefore, assessing whether drivers of forest harvesters and skidders effectively use these permanent skidding trails or not during logging operations can be easily achieved through remote sensing, as we demonstrated here. Thus, airborne LiDAR data provide a promising, although largely untapped, resource to help forest managers monitor whether logging operators respect or ignore the skidding instructions during logging operations.

Soil texture appears as the main determinant explaining the observed variation in CLR (25% of explained variance), together with soil type having a significant effect on the CLR index, which is consistent with former findings showing that soil texture and soil type matter for soil compaction and rutting (Ampoorter et al., 2010; Mohieddinne et al., 2019). More specifically, several studies have shown that soil texture and soil type control soil water-holding capacity, which in turn controls soil compaction and rutting (Ebeling et al., 2016; Hillel, 2004b, 2004c; Lipiec & Håkansson, 2000). The significant decrease in CLR on Gleysols compared to Cambisols is surprising, as these wetland soils are more sensitive to compaction. This difference would therefore be due to silvicultural practices constrained by several specifications, limiting the traffic of machinery onto the plots by adapted practices (e.g., logs extraction using cable skidder, operations restricted to a dry season, etc.). Additionally, we found higher values of the CLR index on acid soils, which suggests that higher soil pH induces a better and faster recovery after compaction, most likely through improved biological activities in the soil (Beylich et al., 2010; Mohieddinne et al., 2019). Moreover, a significantly higher value of the CLR index was found in plots dominated by scots pine compared to plots dominated by beech. The scots pine is preferentially implanted on poor and draining stations, which correspond to the siliceous sand soils in the forest of Compiègne. These acidic and relatively dry soils are hostile to a part of the biodiversity of the soils, in particular the earthworms (Curry, 2004). Consequently, the biological processes helping the recovery of compacted soils could be considerably slowed down, and therefore lead to a longer time persistence of ruts in plots dominated by scots pines.

## 4.2 | How does the rutting index relate to understory plants?

This work presents the first study that assessed the response of understory plant species to a rutting index derived from a remote sensing technique. Several of the examined understory plant species showed an expected response curve along the CLR gradient that we captured from airborne LiDAR, such as *Rumex sanguineus*, *Juncus effusus*, and *Agrostis stolonifera* which responded positively. Previously, Godefroid and Koedam (2004a) reported similarly positive response curves for these three understory plant species along a gradient of soil compaction measured in-situ through soil penetration resistance. Additionally, some studies have already mentioned the occurrence of some understory plant species, especially wetland and ruderal plants like the ones mentioned above, as good bio-indicators of soil

compaction (Kozłowski, 1999; Small & McCarthy, 2002; Weltecke & Gaertig, 2011). Wei et al. (2015) found that the richness of light and moisture-demanding plant species was associated with an increase in bulk density close to skid trails. Similarly, Mercier et al. (2019) found a higher abundance of light and moisture-demanding plant species along skid trails compared to the forest interior. It is widely acknowledged that logging operations in woodlands not only increase light conditions in the understory, thus enhancing the creation of open patches suitable for light-demanding plant species, but it also enhances the creation of superficial waterlogging and pathway habitats, in ruts, suitable for wetland and ruderal plant species (Godefroid & Koedam, 2004b; Mercier et al., 2019; Perry et al., 2008). This is very consistent with our findings of typical wetland and moorland plant species being positively associated with the CLR index (e.g., *Juncus effusus*, *Carex remota*, *Carex pendula*, *Rumex sanguineus*, *Solanum dulcamara*, and *Oxalis acetosella*) (see Figure 2). In parallel, we also found that typical understory plant species associated with dry soils (e.g., *Convallaria majalis* and *Hedera helix*), associated with well-drained soils (e.g., *Viola reichenbachiana* and *Carex flacca*), associated to dry acidic soils (e.g., *Festuca heterophylla*), or associated to shady and dry conditions (e.g., *Luzula forsteri*) respond negatively to an increase in the CLR index. Somewhat consistent with these findings, Closset-Kopp et al. (2019) showed that the increase in forest vehicle traffic is the main reason behind vegetation changes observed over the last decades in the forest of Compiègne. Interestingly, the significant decrease we found in the probability of occurrence of *Quercus petraea* seedlings with CLR may indicate a serious negative impact of forest vehicle traffic on the natural regeneration of this key tree species of high economic value.

As expected, we found canopy density to be negatively correlated with CLR, which is consistent with an increase in light conditions following logging operations. However, and contrary to the species-level responses, we found no correlation between CLR and the floristic indicators aggregated at the community level like species richness or the mean of Ellenberg Indicator Values (EIVs) for soil moisture (EIV-F) across co-occurring species, probably due to the heterogeneity of plant species responses to rutting at the community level. Besides, the indirect effect of rutting and compaction on EIV-F is likely to depend on the spatial heterogeneity in soil conditions (i.e., soil texture and soil type) (Hillel, 2004b), which may blur the direct correlation between CLR and EIV-F. Soil compaction could have a minor influence on coarse soil textures and less biologically active soils (i.e., sandy soils and Podzols). Noteworthy and consistently, when we excluded the plots on sandy soils and Podzols, we found a significantly positive correlation between CLR and EIV-F ( $N = 21$ ,  $p = 0.55$ ,  $p\text{-value} < 0.01$ ). Reduction of the infiltration capacity in compacted soils leads to stagnant waters in fine-textured soils (Herbauts et al., 1996; Hillel, 2004b, 2004c), which favors the occurrence of herbaceous plant species associated with wet conditions, such as *Carex remota*, *Carex pendula*, or *Juncus effusus*. In contrast, the compaction may improve the hydric conditions for coarse-textured soils, like sandy soils, by increasing their water-holding capacity (Hillel, 2004c; Nawaz et al., 2013). Contrary to Mercier et al. (2019), we did not find an increase in species

richness with increasing rutting density. By resurveying old floristic surveys, initially surveyed during the 1970s by Tombal (1972), Closset-Kopp et al. (2019) demonstrated that the heavy traffic of forestry vehicles in the forest of Compiègne led to biotic homogenization of understory plant communities. This biotic homogenization may partially explain why CLR and specific richness are poorly correlated.

## 5 | CONCLUSIONS

In this paper, we proposed the use of a LiDAR-derived rutting index, based on the cumulative length of ruts (CLR), to assess and monitor soil compaction across large spatial extents by means of airborne remote sensing. Like other soil compaction indices proposed in the scientific literature and usually measured in-situ rather than remotely, our CLR index chiefly depends on soil texture and shows expected relationships with several understory plant species that are associated with ruts and thus good bio-indicators of soil compaction, like *Carex remota* or *Juncus effusus*.

Unexpectedly, we found that CLR was greater in forest management units equipped with tagged and permanent skidding trails, suggesting that the tagging of permanent skidding trails by forest managers is not optimal or that logging operators do not really follow the skidding instructions. Yet, the respect of the strict instructions concerning the vulnerability of Gleysols led to prevent the damage, when the lowest CLR is found on this soil type. This emphasizes the need for a systematic method to remotely monitor whether or not logging operators respect the use of permanent skidding trails when available as well as the need for forest managers and logging operators to coordinate closely together to improve the optimization of forest logging operations.

Our findings validate the use of the CLR index as a meaningful index to monitor soil compaction and rutting through remote sensing techniques and thus to assess, remotely, the efficiency of forest management policies. Perspectives for future research include the development of an algorithm to automatically detect ruts from LRM images, which will facilitate the CLR computation and reduce the observer bias. Finally, numerous studies have shown that the intensity of rutting may severely damage soils (Agherkakli et al., 2010; Ampoorter et al., 2010; Bygdén et al., 2003; Sakai et al., 2008). This suggests that an improvement of our index or the creation of a complementary index, considering the magnitude of rutting to distinguish between shallow and deep ruts, could lead to a better assessment of soil rutting and compaction.

## ACKNOWLEDGMENTS

The authors would like to thank the French National Forest Office (ONF) for providing airborne LiDAR images of the studied forest. The authors address their recognition to Augustin Fontenelle for carrying out the botanical surveys. The authors are grateful to Pr. Guillaume Decocq and Dr. Déborah Closset-Kopp, full professor and associate professor, respectively, at the Jules Verne University of Picardy, for their help in achieving the study goal. The authors

would like to thank Dr. Tarek Hattab, research scientist at Ifremer (UMR 248 MARBEC), University of Montpellier, for his help in the study design and for providing LiDAR-derived variables used in this study. The authors thank the anonymous reviewers for their constructive comments.

## CONFLICT OF INTEREST

The authors have no conflict of interest to disclose.

## DATA AVAILABILITY STATEMENT

Our data are available to further and public studies.

## ORCID

Hamza Mohieddinne  <https://orcid.org/0000-0002-9435-0583>

Boris Brasseur  <https://orcid.org/0000-0002-5206-5426>

Jonathan Lenoir  <https://orcid.org/0000-0003-0638-9582>

## REFERENCES

- Agherkakli, B., Najafi, A., & Sadeghi, S. H. (2010). Ground based operation effects on soil disturbance by steel tracked skidder in a steep slope of forest. *Journal of Forest Science*, 56(6), 278–284. <https://doi.org/10.17221/93/2009-JFS>
- Ampoorter, E., Van Nevel, L., De Vos, B., Hermy, M., & Verheyen, K. (2010). Assessing the effects of initial soil characteristics, machine mass and traffic intensity on forest soil compaction. *Forest Ecology and Management*, 260(10), 1664–1676. <https://doi.org/10.1016/j.foreco.2010.08.002>
- Andersen, H. E., Reutebuch, S. E., McGaughey, R. J., d'Oliveira, M. V. N., & Keller, M. (2014). Monitoring selective logging in western Amazonia with repeat LiDAR flights. *Remote Sensing of Environment*, 151, 157–165. <https://doi.org/10.1016/j.rse.2013.08.049>
- Arocena, J. M. (2000). Cations in solution from forest soils subjected to forest floor removal and compaction treatments. *Forest Ecology and Management*, 133, 71–80. <https://doi.org/10.1139/x83-119>
- Augoyard, S., Baron, P., Caco, E., Guilleray, L., Pischedda, D., Helou, T. E., Pousse, N., Ruch, P., & Ulrich, E. (2017). *Pratic sols*. ONF.
- Avon, C., Dumas, Y., & Bergès, L. (2013). Management practices increase the impact of roads on plant communities in forests. *Biological Conservation*, 159, 24–31. <https://doi.org/10.1016/j.biocon.2012.10.008>
- Beatty, S. W. (1984). Influence of microtopography and canopy species on spatial patterns of Forest understory plants. *Ecology*, 65(5), 1406–1419. <https://doi.org/10.2307/1939121>
- Beylich, A., Oberholzer, H.-R., Schrader, S., Höper, H., & Wilke, B.-M. (2010). Evaluation of soil compaction effects on soil biota and soil biological processes in soils. *Soil and Tillage Research*, 109(2), 133–143. <https://doi.org/10.1016/j.still.2010.05.010>
- Blouin, V. M., Schmidt, M. G., Bulmer, C. E., & Krzic, M. (2008). Effects of compaction and water content on lodgepole pine seedling growth. *Forest Ecology and Management*, 255(7), 2444–2452. <https://doi.org/10.1016/j.foreco.2008.01.008>
- Brais, S. (2001). Persistence of soil compaction and effects on seedling growth in northwestern Quebec. *Soil Science Society of America Journal*, 65(4), 1263–1271. <https://doi.org/10.2136/sssaj2001.6541263x>
- BRGM. (2000). Carte Géologique de la France à 1/50000. <http://www.brgm.fr/>
- Burnham, K., & Anderson, D. (2002). *Model selection and multimodel inference. A practical information-theoretic approach* (2nd ed.). New York, NY, USA: Springer. <https://doi.org/10.1177/0049124104268644>
- Bygdén, G., Eliasson, L., & Wästerlund, I. (2003). Rut depth, soil compaction and rolling resistance when using bogie tracks. *Journal of Terramechanics*, 40(3), 179–190. <https://doi.org/10.1016/j.jterra.2003.12.001>

- Callesen, I., Brockmann, B., Fischer, L., Magnussen, A., & Dam, E. B. (2020). *Wheel rutting: Preliminary investigations of soil redox potential and automated monitoring of their presence using machine learning and highresolution LiDAR data* (pp. 58–62). Session 3– Impact and Organization. [https://ign.ku.dk/english/employees/all-employees-ign/?pure=en%2Fpublications%2Fwheel-rutting-preliminary-investigations-of-soil-redox-potential-and-automated-monitoring-of-their-presence-using-machine-learning-and-highresolution-lidar-data\(cbf4e33d-daa7-402f-857b-24430e02f6dc\).html](https://ign.ku.dk/english/employees/all-employees-ign/?pure=en%2Fpublications%2Fwheel-rutting-preliminary-investigations-of-soil-redox-potential-and-automated-monitoring-of-their-presence-using-machine-learning-and-highresolution-lidar-data(cbf4e33d-daa7-402f-857b-24430e02f6dc).html)
- Cambi, M., Certini, G., Neri, F., & Marchi, E. (2015). The impact of heavy traffic on forest soils: A review. *Forest Ecology and Management*, 338, 124–138. <https://doi.org/10.1016/j.foreco.2014.11.022>
- Cambi, M., Giannetti, F., Bottalico, F., Travaglini, D., Nordfjell, T., Chirici, G., & Marchi, E. (2018). Estimating machine impact on strip roads via close-range photogrammetry and soil parameters: A case study in Central Italy. *iForest*, 11, 148–154. <https://doi.org/10.3832/ifer2590-010>
- Cambi, M., Hoshika, Y., Mariotti, B., Paoletti, E., Picchio, R., Venanzi, R., & Marchi, E. (2017). Compaction by a forest machine affects soil quality and *Quercus robur* L. seedling performance in an experimental field. *Forest Ecology and Management*, 384, 406–414. <https://doi.org/10.1016/j.foreco.2016.10.045>
- Cambi, M., Mariotti, B., Fabiano, F., Maltoni, A., Tani, A., Foderi, C., & Marchi, E. (2018). Early response of *Quercus robur* seedlings to soil compaction following germination. *Land Degradation & Development*, 29(4), 916–925. <https://doi.org/10.1002/ldr.2912>
- Climate-data.org. (2019). *Climate data*. Consulté 20 février, à l'adresse <https://fr.climate-data.org/>
- Closset-Kopp, D., Hattab, T., & Decocq, G. (2019). Do drivers of forestry vehicles also drive herb layer changes (1970–2015) in a temperate forest with contrasting habitat and management conditions? *Journal of Ecology*, 107(3), 1439–1456. <https://doi.org/10.1111/1365-2745.13118>
- Curry, J. P. (2004). Factors affecting the abundance of earthworms in soils. In C. A. Edwards (Ed.), *Earthworm ecology* (2nd ed., pp. 263–286). Boca Raton, FL, USA: CRC Press.
- d'Oliveira, M. V. N., Reutebuch, S. E., McGaughey, R. J., & Andersen, H. E. (2012). Estimating forest biomass and identifying low-intensity logging areas using airborne scanning LiDAR in Antimary State Forest, Acre State, Western Brazilian Amazon. *Remote Sensing of Environment*, 124, 479–491. <https://doi.org/10.1016/j.rse.2012.05.014>
- Ebeling, C., Lang, F., & Gaertig, T. (2016). Structural recovery in three selected forest soils after compaction by forest machines in Lower Saxony, Germany. *Forest Ecology and Management*, 359, 74–82. <https://doi.org/10.1016/j.foreco.2015.09.045>
- Godefroid, S., & Koedam, N. (2004a). Interspecific variation in soil compaction sensitivity among forest floor species. *Biological Conservation*, 119, 207–217. <https://doi.org/10.1016/j.biocon.2003.11.009>
- Godefroid, S., & Koedam, N. (2004b). The impact of forest paths upon adjacent vegetation: Effects of the path surfacing material on the species composition and soil compaction. *Biological Conservation*, 119(3), 405–419. <https://doi.org/10.1016/j.biocon.2004.01.003>
- Goutal, N., Boivin, P., & Ranger, J. (2012). Assessment of the natural recovery rate of soil specific volume following forest soil compaction. *Soil Science Society of America Journal*, 76(4), 1426–1435. <https://doi.org/10.2136/sssaj2011.0402>
- Greacen, E. L., & Sands, R. (1980). Compaction of forest soils. A review. *Australian Journal of Soil Research*, 18(2), 163–189. <https://doi.org/10.1111/j.1574-6941.2006.00175.x>
- Grigal, D. F. (2000). Effects of extensive forest management on soil productivity. *Forest Ecology and Management*, 138, 167–185. [https://doi.org/10.1016/S0378-1127\(00\)00395-9](https://doi.org/10.1016/S0378-1127(00)00395-9)
- Haas, J., Hagge Ellhöft, K., Schack-Kirchner, H., & Lang, F. (2016). Using photogrammetry to assess rutting caused by a forwarder—a comparison of different tires and bogie tracks. *Soil and Tillage Research*, 163, 14–20. <https://doi.org/10.1016/j.still.2016.04.008>
- Hamza, M. A., & Anderson, W. K. (2005). Soil compaction in cropping systems: A review of the nature, causes and possible solutions. *Soil and Tillage Research*, 82(2), 121–145. <https://doi.org/10.1016/j.still.2004.08.009>
- Hattab, T., Garzón-López, C. X., Ewald, M., Skowronek, S., Aerts, R., Horen, H., Brasseur, B., Gallet-Moron, E., Spicher, F., Decocq, G., Feilhauer, H., Honnay, O., Kempeneers, P., Schmidtlein, S., Somers, B., Van De Kerchove, R., Rocchini, D., & Lenoir, J. (2017). A unified framework to model the potential and realized distributions of invasive species within the invaded range. *Diversity and Distributions*, 23(7), 806–819. <https://doi.org/10.1111/ddi.12566>
- Herbauts, J., El Bayad, J., & Gruber, W. (1996). Influence of logging traffic on the hydromorphic degradation of acid forest soils developed on loessic loam in middle Belgium. *Forest Ecology and Management*, 87(1–3), 193–207. [https://doi.org/10.1016/S0378-1127\(96\)03826-1](https://doi.org/10.1016/S0378-1127(96)03826-1)
- Hesse, R. (2010). LiDAR-derived local relief models—A new tool for archaeological prospection. *Archaeological Prospection*, 17, 61–62. <https://doi.org/10.1002/arp>
- Hillel, D. (2004a). Stress, strain, and strength of soil bodies. In D. Hillel (Ed.), *Introduction to environmental soil physics* (pp. 235–255). Elsevier. <https://doi.org/10.1016/B978-012348655-4/50014-9>
- Hillel, D. (2004b). Water entry into soil. In D. Hillel (Ed.), *Introduction to environmental soil physics* (pp. 259–282). Elsevier. <https://doi.org/10.1016/B978-012348655-4/50015-0>
- Hillel, D. (2004c). Redistribution and retention of soil moisture. In D. Hillel (Ed.), *Introduction to environmental soil physics* (pp. 297–313). Elsevier. <https://doi.org/10.1016/B978-012348655-4/50017-4>
- Horn, R., Vossbrink, J., Peth, S., & Becker, S. (2007). Impact of modern forest vehicles on soil physical properties. *Forest Ecology and Management*, 248(1–2), 56–63. <https://doi.org/10.1016/j.foreco.2007.02.037>
- Hurvich, C., & Tsai, C.-L. (1989). Regression and time series model selection in small samples. *Biometrika*, 76, 297–307. <https://doi.org/10.1093/biomet/76.2.297>
- Jansson, K.-J., & Johansson, J. (1998). Soil changes after traffic with a tracked and a wheeled forest machine: A case study on a silt loam in Sweden. *Forest*, 71(1), 57–66. <https://doi.org/10.1093/forestry/71.1.57>
- Koreň, M., Slančík, M., Suchomel, J., & Dubina, J. (2015). Use of terrestrial laser scanning to evaluate the spatial distribution of soil disturbance by skidding operations. *iForest*, 8, 386–393. <https://doi.org/10.3832/ifer1165-007>
- Kozłowski, T. T. (1999). Soil compaction and growth of woody plants. *Scandinavian Journal of Forest Research*, 14, 596–619. <https://doi.org/10.1080/02827589908540825>
- Lipiec, J., & Håkansson, I. (2000). Influences of degree of compactness and matric water tension on some important plant growth factors. *Soil and Tillage Research*, 53(2), 87–94. [https://doi.org/10.1016/S0167-1987\(99\)00094-X](https://doi.org/10.1016/S0167-1987(99)00094-X)
- Marra, E., Cambi, M., Fernandez-Lacruz, R., Giannetti, F., Marchi, E., & Nordfjell, T. (2018). Photogrammetric estimation of wheel rut dimensions and soil compaction after increasing numbers of forwarder passes. *Scandinavian Journal of Forest Research*, 33(6), 613–620. <https://doi.org/10.1080/02827581.2018.1427789>
- Mercier, P., Aas, G., & Dengler, J. (2019). Effects of skid trails on understory vegetation in forests: A case study from northern Bavaria (Germany). *Forest Ecology and Management*, 453, 117579. <https://doi.org/10.1016/j.foreco.2019.117579>
- Meyer, C., Lüscher, P., & Schulin, R. (2014). Recovery of forest soil from compaction in skid tracks planted with black alder [*Alnus glutinosa* (L.) Gaertn.]. *Soil and Tillage Research*, 143, 7–16. <https://doi.org/10.1016/j.still.2014.05.006>
- Mohieddinne, H., Brasseur, B., Spicher, F., Gallet-Moron, E., Buridant, J., Kobaissi, A., & Horen, H. (2019). Physical recovery of forest soil after compaction by heavy machines, revealed by penetration resistance



- over multiple decades. *Forest Ecology and Management*, 449, 117472. <https://doi.org/10.1016/J.FORECO.2019.117472>
- Mueller-Dombois, D., & Ellenberg, H. (1974). *Aims and methods of vegetation ecology*. New York, NY, USA: Wiley.
- Nawaz, M. F., Bourri , G., & Trolard, F. (2013). Soil compaction impact and modelling. A review. *Agronomy for Sustainable Development*, 33(2), 291–309. <https://doi.org/10.1007/s13593-011-0071-8>
- Niemi, M. T., Vastaranta, M., Vauhkonen, J., Melkas, T., & Holopainen, M. (2017). Airborne LiDAR-derived elevation data in terrain trafficability mapping. *Scandinavian Journal of Forest Research*, 32(8), 762–773. <https://doi.org/10.1080/02827581.2017.1296181>
- ONF. (2012). *R vision d'am nagement forestier 2012–2031. For t domaniale de Compi gne*. Agronomic and Agriculture Minister, France Republic.
- Pardo, A., Amato, M., & Chiarand , F. Q. (2000). Relationships between soil structure, root distribution and water uptake of chickpea (*Cicer arietinum* L.). plant growth and water distribution. *European Journal of Agronomy*, 13(1), 39–45. [https://doi.org/10.1016/S1161-0301\(00\)00056-3](https://doi.org/10.1016/S1161-0301(00)00056-3)
- Perry, D., Oren, R., & Hart, S. (2008). *Forest ecosystem* (2nd ed.). Baltimore, MD, USA: Johns Hopkins University Press.
- Pierzcha a, M., Talbot, B., & Astrup, R. (2016). Measuring wheel ruts with close-range photogrammetry. *Forestry*, 89(4), 383–391. <https://doi.org/10.1093/forestry/cpw009>
- R Development Core Team. (2016). *R: A language and environment for statistical computing*. Vienna, AT: Foundation for Statistical Computing.
- Sakai, H., Nordfjell, T., Suadicani, K., Talbot, B., & B llehuus, E. (2008). Soil compaction on forest soils from different kinds of tires and tracks and possibility of accurate estimate. *Croatian Journal of Forest Engineering*, 29(1). <https://www.semanticscholar.org/paper/Soil-Compaction-on-Forest-Soils-from-Different-of-Sakai-Nordfjell/9a2818228e1eeb79de7b70d96b4af8c06509465a>
- Salmivaara, A., Miettinen, M., Fin r, L., Launiainen, S., Korpunen, H., Tuominen, S., Heikkonen, J., Nevalainen, P., Sir n, M., Ala-Ilom ki, J., & Uusitalo, J. (2018). Wheel rut measurements by forest machine-mounted LiDAR sensors – Accuracy and potential for operational applications? *International Journal of Forest Engineering*, 29(1), 1–12. <https://doi.org/10.1080/14942119.2018.1419677>
- Schumacher, T. E., & Smucker, A. J. M. (1981). Mechanical impedance effects on oxygen uptake and porosity of drybean roots 1. *Agronomy Journal*, 73(1), 51–55. <https://doi.org/10.2134/agronj1981.00021962007300010012x>
- Slesak, R. A., & Kaebisch, T. (2016). Using lidar to assess impacts of forest harvest landings on vegetation height by harvest season and the potential for recovery over time. *Canadian Journal of Forest Research*, 46(6), 869–875. <https://doi.org/10.1139/cjfr-2015-0517>
- Small, C. J., & McCarthy, B. C. (2002). Effects of simulated post-harvest light availability and soil compaction on deciduous forest herbs. *Canadian Journal of Forest Research*, 32(10), 1753–1762. <https://doi.org/10.1139/x02-099>
- Talbot, B., Rahlf, J., & Astrup, R. (2018). An operational UAV-based approach for stand-level assessment of soil disturbance after forest harvesting. *Scandinavian Journal of Forest Research*, 33(4), 387–396. <https://doi.org/10.1080/02827581.2017.1418421>
- Tombal, P. (1972). Recherches sur les potentialit s phytoc enologiques de la for t de Compi gne (Oise–France). *Bulletin de la Soci t  Botanique du Nord de la France*, 25, 31–52.
- Wei, L., Villemey, A., Hulin, F., Bilger, I., Yann, D., Chevalier, R., Archaux, F., & Gosselin, F. (2015). Plant diversity on skid trails in oak high forests: A matter of disturbance, micro-environmental conditions or forest age? *Forest Ecology and Management*, 338, 20–31. <https://doi.org/10.1016/j.foreco.2014.11.018>
- Weltecke, K., & Gaertig, T. (2011). Methods for the assessment of soil deformation in forest stands: Interrelationships and ecological relevance. *German Journal of Forest Research*, 182(9/10), 187–204. [http://www.sauerlaender-verlag.com/CMS/fileadmin/content/dokument/archiv/afjz/182\\_2011/Heft5/\\_02\\_Weltecke\\_6147.pdf](http://www.sauerlaender-verlag.com/CMS/fileadmin/content/dokument/archiv/afjz/182_2011/Heft5/_02_Weltecke_6147.pdf)
- Zenner, E. K., & Berger, A. L. (2008). Influence of skidder traffic and canopy removal intensities on the ground flora in a clearcut-with-reserves northern hardwood stand in Minnesota, USA. *Forest Ecology and Management*, 256(10), 1785–1794. <https://doi.org/10.1016/j.foreco.2008.05.030>

## SUPPORTING INFORMATION

Additional supporting information can be found online in the Supporting Information section at the end of this article.

**How to cite this article:** Mohieddinne, H., Brasseur, B., Gallet-Moron, E., Lenoir, J., Spicher, F., Kobaissi, A., & Horen, H. (2023). Assessment of soil compaction and rutting in managed forests through an airborne LiDAR technique. *Land Degradation & Development*, 34(5), 1558–1569. <https://doi.org/10.1002/ldr.4553>